Journal of Industrial Microbiology & Biotechnology (1998) 21, 261–274

http://www.stockton-press.co.uk/jim

Community structure of biofilms on ennobled stainless steel in Baltic Sea water

M Kolari, K Mattila, R Mikkola and MS Salkinoja-Salonen

University of Helsinki, Department of Applied Chemistry and Microbiology, PO Box 56, FIN-00014 University of Helsinki, Finland

Stainless steel samples (AISI 316) were ennobled in a laboratory simulator with natural Baltic Sea water. After completion of ennoblement (increase of open circuit potential of *ca* 400 mV), the biofilm on the steel surface was characterized using confocal laser scanning microscopy (CLSM) in combination with functional and phylogenetic stains. The biofilm consisted of microbial cell clusters covering 10–20% of the surface. The clusters were loaf-formed, with a basal diameter of 20–150 μm, 5–20 per mm^{-2}, each holding $>10^4$ cells in a density of 1–5 $\times$ 10^7 cells mm^{-3}. The typical cluster contained mainly small Gram-negative bacteria (binding the EUB338 probe when hybridized *in situ* on the steel surface), and often carried one to three spherical colonies, either homogeneously composed of large Gram-negative cocci or more often small bacterial rods in high density, 10^8–10^9 cells mm^{-3}. The clusters in live biofilms contained no pores, and clusters over 25 μm in diameter had a core nonpenetrable to fluorescent nucleic acid stains and ConA lectin stain. Fluorescently-tagged ConA stained cells at a depth of <5 μm, indicating the presence of cells with α-D-mannosyl and α-D-glucosyl residues on surfaces. Ethidium bromide (log K_{ow} –0.38) penetrated deeper (17 μm in 15 min, corresponding to >10 cells in a stack) into the cluster than did the less polar dyes SYTO 16 (log K_{ow} 1.48) and acridine orange (log K_{ow} 1.24), which stained five cells in a stack. Fluorescent hydrophobic and hydrophilic latex beads (diameter 0.02, 0.1 or 1.0 μm) coated patchwise the cluster surface facing the water, but penetrated only to depths of $\leqslant$2 μm indicating a permeability barrier. About 1/3 of the stainable cells hybridized *in situ* with Alf1b, while fewer than 1/7 hybridized to GAM42, probes targeted towards α- and γ-*Proteobacteria*, respectively. Our results represent a microscopic description of an ennobling biofilm, where the ennoblement could follow the sequence of redox events as suggested by the model of Dickinson and Lewandowski (1996) for the structure of corrosive biofilms on a steel surface.

Keywords: biofilms; stainless steel; Baltic Sea; ennoblement; CLSM; *in situ* hybridization; fluorescent beads

Introduction

Biofilm formation on stainless steel surfaces may contribute to microbially influenced corrosion [6]. The role of biofilms in the corrosion of stainless steel in marine applications has been dealt with in numerous studies but is only partially understood. Ennobling, ie the increase of the free corrosion potential of stainless steel in the passive state by 100–400 mV is known to occur during biofilm growth on stainless steel surfaces in all European seas [4].

The causative relationship between the biology (the biofilm formation) and the electrochemistry (the increase in E_{corr}) is unclear. Mollica [34] observed no ennoblement in sea water where the microbes had previously been removed by filtration, supporting the hypothesis that biofilm formation is required for ennoblement. One difficulty in studies of the biology of ennoblement has been that it has been difficult to reproduce under controlled laboratory conditions.

We recently demonstrated a laboratory ecosystem where the ennoblement of stainless steel occurred in an electrochemical sequence of events identical to that observed under field conditions in the Baltic Sea [33]. This opened the possibility of analyzing under laboratory conditions the structure of biofilms emerging on ennobling stainless steel surfaces. CLSM and non-aggressive tools, fluorochromes and fluorescent latex beads of different sizes and surface properties were used to study the structure and barrier properties of biofilms on ennobled stainless steel. Live Gram-staining and *in situ* hybridization with fluorescently labeled rRNA targeting probes were used to characterize the biofilm population.

Correspondence: M Kolari, University of Helsinki, Department of Applied Chemistry and Microbiology, PO Box 56 (Biocenter, Viikinkaari 9), FIN-00014 University of Helsinki, Finland
Received 14 January 1998; accepted 18 July 1998

Materials and methods

Propagation of biofilms on ennobling stainless steel

Coupons of stainless steel (AISI 306, Ø 13 mm) were polished to 600 grit and mounted in a Robbins device in a laboratory model ecosystem [33]. Natural Baltic Sea water collected from the Helsinki coastal area (brackish, salinity 0.5%, pH 7.3–7.9, DOC 4–7 mg L^{-1}, total N 310–1100 μg L^{-1}, total P 24–38 μg L^{-1}, Cl^- 2800–3000 mg L^{-1}, Fe 80–240 μg L^{-1}, Ca 81–86 mg L^{-1}, SO^{2-}_4 510–530 mg L^{-1}, Al 60–400 μg L^{-1}, Mn 30–80 μg L^{-1}) was recycled between the light (100 L, 1850 lux, 12 h day^{-1}) and the dark (25 L) compartments at room temperature (23 ± 1°C). The feeding rate was 0.05 day^{-1} and the hydraulic flow facing the steel coupons in the dark compartment was adjusted to 30 ± 5 mm s^{-1}. With these operational parameters a steady state was achieved, where the levels of dissolved oxygen (close to saturation), TOC and different forms of nitrogen

in the laboratory ecosystem were maintained identical to those in the Baltic Sea [33]. The open circuit potentials of the coupons were measured using a potentiostat (Wenking LB81M, Clausthal, Germany) with saturated calomel electrode (SCE) as the reference electrode, as described by Carpén *et al* [10].

In situ hybridization

The stainless steel coupons with biofilms were rinsed with sterile water, air-dried and stored desiccated at room temperature. Table 1 describes the oligonucleotide probes used. The probes were purchased from MWG-Biotech, Ebersberg, Germany. Microbes with target rRNA sequences for the oligonucleotide probes shown in Table 2 were searched from the Ribosomal Database Project (release 27.6.97 [31]) and from the GenEMBL (division Bacterial, release 6/97). The matches from GenEMBL were retrieved and compared using programs Fasta, Fetch and Findpatterns of the Wisconsin Package Program v. 9.0 (Genetics Computer Group, Madison, WI, USA).

Air-dried stainless steel coupons were pretreated with ethanol:30% aqueous formaldehyde (90:10 v/v) for 5 min, rinsed with sterile water and excess water was removed (protocol modified from [8]). The ethanol-formaldehyde treatment was used to reduce nonspecific fluorescence [1]. The hybridization mixture contained 20–35% formamide (Table 1) to ensure hybridization stringency, 62.5 ng of each probe in 20 μl, 0.9 M NaCl, 20 mM Tris-HCl pH 7.2 and 0.01% SDS [32]. Twenty microliters of this mixture were applied on the steel coupon and incubated for 2 h at 46°C in a humidity chamber. The unbound probe was removed from the coupons with 2 ml of washing solution: 20 mM Tris, 0.01% SDS and 5 mM EDTA and 40–180 mM NaCl (Table 1). The coupons were then immersed in 50 ml of the washing solution at 48°C for 20 min, rinsed briefly with sterile water and microscopically inspected after air-drying.

The staining procedure for living biofilms

The stainless steel coupons were immersed in Baltic Sea water until the ennoblement was completed and stored briefly in stagnant Baltic Sea water at 4°C in the dark until stained just prior to examination. The stains used are listed in Table 2. The staining mixture contained one red and one green fluorescing dye in 5 ml of Baltic Sea water in a 15-ml polypropylene tube. The staining mixture was vigorously vortexed for 45 s before the stainless steel coupon was squeezed firmly in the tube into a horizontal position with the biofilm side facing down (Figure 1a). The coupons were maintained in the horizontal position with the biofilm coated surface down to avoid sedimentation of materials during the incubation of 15 min on a rotary shaker (150 rpm) at 28°C. The stained coupons were then rinsed twice for 3 min by immersion in flowing Baltic Sea water and moved into clean polypropylene tubes filled with Baltic Sea water. For sequential staining the coupons were stained with two dyes, 10 min each.

The fluorescent stains used

Latex microbead suspensions were sonicated prior to dilution in Baltic Sea water and microscopically checked, to assure that the beads were in a monodispersed state. Carboxylate-modified FluoSpheres® beads are highly uniform sulfate latex microspheres with pendent carboxylic acid groups, hydrophilic and moderately or highly charged (Table 2). Aldehyde sulfate FluoSpheres® beads are sulfate microspheres with added aldehyde groups on surfaces, hydrophobic and weakly charged (Table 2), binding to hydrophobic surfaces and molecules [21]. Three cell-permeant nucleic acid stains were used, SYTO™ 16, ethidium bromide (EtBr) and acridine orange, all positively charged at neutral pH. SYTO™ 16 stock solution was thawed before use and briefly microcentrifuged to deposit the dimethylsulfoxide solvent at the bottom of the vial. The supernatant phase was diluted 100× with Baltic Sea water for staining. Ethidium bromide stock solution in water was diluted 100× with Baltic Sea water for use. Acridine orange was used singly, because of the broad fluorescence emission spectrum (see Table 2). The stock solution in water was diluted 100× with Baltic Sea water for use. Concanavalin A lectin conjugated with tetramethylrhodamine fluorophore (ConA-TRITC) was used to indicate polysaccharides (binds to α-mannopyranosyl and α-glucopyranosyl residues). In alkaline and neutral conditions it occurs as a tetramer of approx. 104 000 g mol^{-1} [21]. It was used as solution of 1 mg ml^{-1} in 0.1 M sodium bicarbonate, pH 8.5, containing 1 mM of Mg^{2+} and 1 mM of Ca^{2+}, thawed and briefly microcentrifuged before use to eliminate aggregates. The live Gram-stain used was LIVE BacLight Bacterial Gram Stain Kit consisting of two components: SYTO 9 to stain living Gram-negative bacteria (green fluorescence) and hexidium iodide to stain living Gram-positive bacteria (red fluorescence). Hexidium iodide also stains dead bacteria and eucaryotes. Both stock solutions were applied to the specimen 1.5 μl ml^{-1} under stagnant conditions in the dark and incubated for 15 min with no wash steps before microscopy. Dyes were purchased from Molecular Probes

Table 1 Oligonucleotide probes and the experimental conditions used for *in situ* hybridizations with the biofilms on ennobled stainless steel

Probe	Sequence	Target site (*E. coli* rRNA numbering)	Specific for	Label	% Formamide (hybridization)	NaCl (mM) (washing)
EUB338	5′-GCTGCCTCCCGTAGGAGT-3′	16S (338–355)	domain *Bacteria*[a]	fluorescein	20	180
ALF1b	5′-CGTTCG(C/T)TCTGAGCCAG-3′	16S (19–35)	alpha *Proteobacteria*[a,b]	Cy3	20	180
GAM42a	5′-GCCTTCCCACATCGTTT-3′	23S (1027–1043)	gamma *Proteobacteria*[a]	Cy3	35	40

[a]Described by Manz *et al* [32].
[b]ALF1b also binds some organisms of the delta subclass of *Proteobacteria* and some Gram-positive bacteria with a low G+C content of DNA [32].

Table 2 Properties of the fluorescent stains used in the CLSM studies of the stainless steel biofilms

Fluorescent stain	Diameter or molecular weight	Concentration of the staining solution	Surface properties	Surface charge	Excitation max.[a]	Emission max.[b]
Fluorescent beads[c]						
Carboxylate-modified FluoSpheres® (CM)	1.0 μm (1.01 μm ± 2.5%)	7.0×10^7 beads ml^{-1}	hydrophilic	negative (219 μC cm^{-2})	580	605
Carboxylate-modified FluoSpheres®	0.1 μm (0.093 μm ± 7.4%)	4.5×10^{10} beads ml^{-1}	hydrophilic	negative (102 μC cm^{-2})	505	515
Carboxylate-modified FluoSpheres®	0.02 μm (0.02 μm ± 15.8%)	4.5×10^{12} or 9.0×10^{12} beads ml^{-1}	hydrophilic	negative (16.1 μC cm^{-2})	580	605
Aldehyde-sulfate FluoSpheres® (AS)	0.02 μm (0.029 μm ± 20.1%)	1.5×10^{12} or 3.0×10^{12} beads ml^{-1}	hydrophobic	negative (4.2 μC cm^{-2})	505	515
Nucleic acid stains						
Acridine orange (AO)	302 g mol^{-1}	100 μg ml^{-1}	log K_{ow} 1.24	positive	500 (DNA) 460 (RNA)	526 (DNA) 650 (RNA)
Ethidium bromide (EtBr)	394 g mol^{-1}	100 μg ml^{-1}	log K_{ow} –0.38	positive	518	605
SYTO™ 16	~450[d] g mol^{-1}	10 μM	log K_{ow} 1.48	positive	488	518
Miscellaneous stains						
Concanavalin A, tetramethylrhodamine conjugate (ConA-TRITC)	104 000 g mol^{-1}	200 μg ml^{-1}	hydrophilic	negative	541	572

[a]Fluorescence excitation maxima (nm).
[b]Fluorescence emission maxima (nm).
[c]According to the manufacturer, prepared by a surfactant-free process and stored in ultrapure water.
[d]Exact data not available (proprietary information).

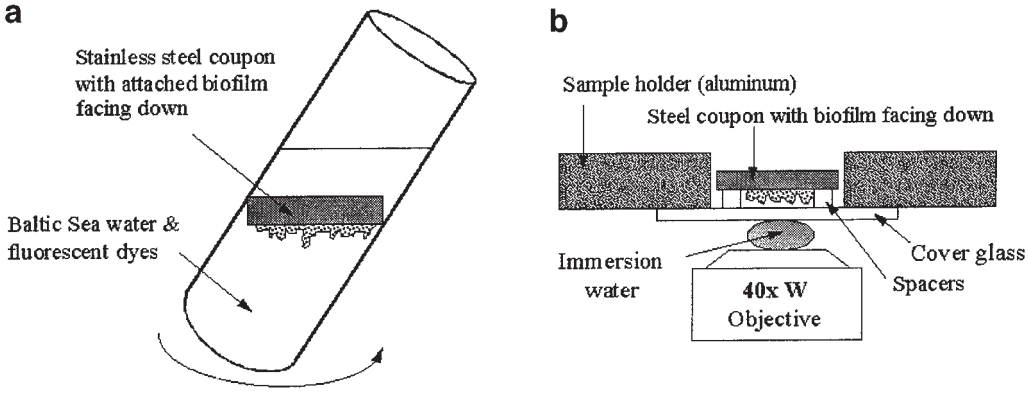

Figure 1 The experimental setup for studying the penetration of dyes into the biofilms on ennobled stainless steel. (a) Steel coupons were inserted firmly into polypropylene tubes filled with Baltic Sea water, dyes were added and the whole was incubated 15 min on a shaker rotating laterally at 150 rpm. (b) For CLSM examination the coupons were mounted in a holder.

Europe (Leiden, The Netherlands) except for EtBr (Pharmacia Biotech AB, Uppsala, Sweden).

Partition coefficient (octanol:water) estimation by RP-HPLC

The *n*-octanol : water partition coefficient (log K_{ow}) for SYTO 16 was estimated as described in ASTM Standard E 1147-92 [3] using Nova-Pak C18 column, 3.9 mm × 300 mm, 4 μm (Waters Co, Milford, MA, USA). The eluent was methanol/water (50:50 v/v), the flow rate was 0.6 ml min^{-1} and detection was at 254 nm. The reference compounds used for calibration were naphthol (calculated log K_{ow} 2.69), indoline (log K_{ow} 2.05) and 7-hydroxymethylcoumarin (log K_{ow} 1.58; Sigma Chemicals Co, St Louis, MO, USA). An internal standard was sodium nitrate (E Merck, Darmstadt, Germany).

Bacterial strains used

Strains *Mycobacterium gadium* NCTC 10942^T and *Deinococcus geothermalis* RSPS-7a were used to check dye penetration. Strain *Mycobacterium gadium* NCTC 10942^T was obtained from the National Collection of Type Cultures, Central Public Health Laboratory, London, UK. *Deinococcus geothermalis* RSPS-7a [15] was kindly provided by Milton DaCosta from the Department of Biochemistry, University of Coimbra, Portugal.

Scanning electron microscopy (SEM)

For SEM analysis, the stainless steel coupons were rinsed with sterile water and fixed in 3% glutaraldehyde (w/v, Merck, Munich, Germany) in Sörensen phosphate buffer (1/15 M, pH 7.2; KH_2PO_4–Na_2HPO_4) for 2 h. The coupons were rinsed three times with the buffer, dehydrated in a

series of 40–100% of ethanol (five steps, 15 min in each), critical point dried and gold coated. The coupons were examined with a scanning electron microscope (JSM-840, Jeol, Tokyo, Japan) at voltages of 5–15 kV.

Confocal laser scanning microscopy (CLSM)

A BioRad MCR-1024 confocal laser scanning system with inverted Zeiss Axiovert 135 M light microscope was used with 488 and 568-nm excitation lines of a KrAr-laser (3% of the maximum 15 mW), emission filters BP 515–525 nm and EFLP 580 nm and pinholes of 2.0 mm. For mounting the steel coupons with living biofilms a sample holder as shown in Figure 1b was used. The sample holder was filled with distilled water and 170-μm thick pieces of coverglass were used as spacers to prevent compression of the biofilm. The coupons with living biofilms were examined with a 40× water immersion objective (Zeiss C-Apochromat, N.A. 1.2, Oberkochen, Germany). The coupons with *in situ* hybridized biofilms were mounted without spacers, immersed into SlowFade™ antibleach media (Molecular Probes, Eugene, OR, USA) and examined with a 63× oil immersion objective (Zeiss Plan-Apochromat, N.A. 1.4 DIC, Oberkochen, Germany).

Image collection was performed with the Lasersharp v. 2.1A software (Bio-Rad, Hemel Hempstead, UK). Background fluorescence was evaluated from unstained samples and eliminated by the choice of collection parameters used with CLSM. Image combining and processing were performed with ImageSpace™ v. 3.20 (Molecular Dynamics, Sunnyvale, CA, USA) image analysis program run in an Indigo 2 workstation (Silicon Graphics, Mountain View, CA, USA). Stain penetration into clusters was measured from single optical *xy*-sections of the stained biofilms with the 2-D distance measurement option of the ImageSpace™ software.

Results

Structure of the living biofilms on ennobling stainless steel

Stainless steel coupons were exposed to Baltic sea water in a laboratory ecosystem, where ennobling of the stainless steel occurred similarly to field conditions (increase in open circuit potentials approx. 400 mV in 3–4 weeks). The ennobled stainless steel coupons were inspected with a confocal laser scanning microscope (CLSM) shortly after removal from the Baltic Sea simulator. CLSM images of a living biofilm on a stainless steel coupon ennobled in Baltic Sea water, after staining with ethidium bromide (EtBr) and fluorescent latex beads of 0.02 μm diameter, are shown in Figure 2. It shows that a 66-μm high cell cluster was packed with EtBr stained (red) rod-shaped cells in a density of 1–5 $\times$ 10^7 mm^{-3} and a few filamentous bacteria. The cluster extruded like a mountain from the metal surface towards the flowing Baltic Sea water and its summit formed a thin >20-μm long streamer, floating freely with water currents. The green color in Figure 2 reveals the location of the 0.02-μm aldehyde sulfate latex beads. Panels (b–d) of Figure 2 represent partial *xy*-projections, revealing parts of the cell cluster 46, 26 and 10 μm distal to the steel surface. Projections show that the beads were located as peripheral patches in the cluster, in contrast to EtBr which had uniformly penetrated all cells to a depth of 17 μm (Table 3). EtBr also did not stain the interior of the cluster. The lack of penetration of EtBr as well as that of the beads is clearly visible in panel (d), displaying the sum of 10 μm most proximal to the metal surface.

Figure 3 shows *z*-profiles of the cluster shown in Figure 2 as *xy*-projections. Each of the three panels represents a 10-μm thick vertical slice of the cluster. The voids and cavities in the biofilm are visualized by the aldehyde sulfate beads (0.02 μm) in the top panel, showing exclusion of the beads from the cluster interior and penetration only in the cluster periphery to a depth of a few μm. No voids deeper than 5 μm were penetrated by the fluorescent beads, thus there was no transport of beads via water flow into cavities of the interior of the cluster. The penetration of EtBr into the biofilm is shown in the middle panel of Figure 3. The unstained core most proximal to the steel surface represented 1/4 of the volume of the cluster. Figure 4 shows biofilm development on stainless steel as seen with SEM. Panel (a) shows morphologically different bacteria attached to the steel surface during the first 22 days of immersion in Baltic Sea water. Bacteria resembling eg *Seliberia*, *Hyphomonas* and *Caulobacter* are seen. Panel (b) shows the steel surface 27 days after ennoblement occurred (immersion of 56 days). Cell clusters had grown from some but not all adherent bacteria, to a diameter of 20–100 μm (not corrected for shrinkage caused by drying), scattered patchwise over the steel surface, covering ~20% of the surface area.

Based on results, of which examples are shown in Figures 2 and 3 (CLSM) and Figure 4 (SEM), the basic features of the laboratory-grown Baltic Sea biofilms on stainless steel 10–15 days after completion of the ennoblement, were as follows. The steel was partially covered with clusters 15–20 mm^{-2}, each with a basal diameter of 20–150 μm. These clusters consisted of densely packed bacterial cells, visible after staining with EtBr, in a density of 1–5 $\times$ 10^7 cells mm^{-3}. Clusters with a basal diameter around 100 μm were calculated to contain 0.5–1.5 $\times$ 10^4 cells each. The steel surface adjacent to the clusters was either bare, covered with a few cells embedded in a thin film as shown in Figure 4 or with single attached cells, mostly short rods. After eliminating background fluorescence, only the following objects were detected by their autofluorescence from unstained samples: (i) cyanobacterial filaments and with a low frequency; (ii) nematodes; and (iii) diatoms. Brightly autofluorescing, possibly non-living particles ~1 μm in diameter, were detected with a low frequency corresponding to less than 0.01% of the stainable bacterial cells.

Penetration of fluorescent dyes into the cell clusters

The depth of penetration of dyes into the clusters of the biofilm on stainless steel ennobled in the Baltic Sea was measured from the optical *xy*-sections collected by CLSM. Comparisons of the penetration between the primary and secondary stain done from the same cluster, stained simultaneously, as shown in Table 3. Three different nucleic acid dyes with similar molecular weights were used. EtBr penetrated deepest, up to 17 μm below the cluster surface. EtBr

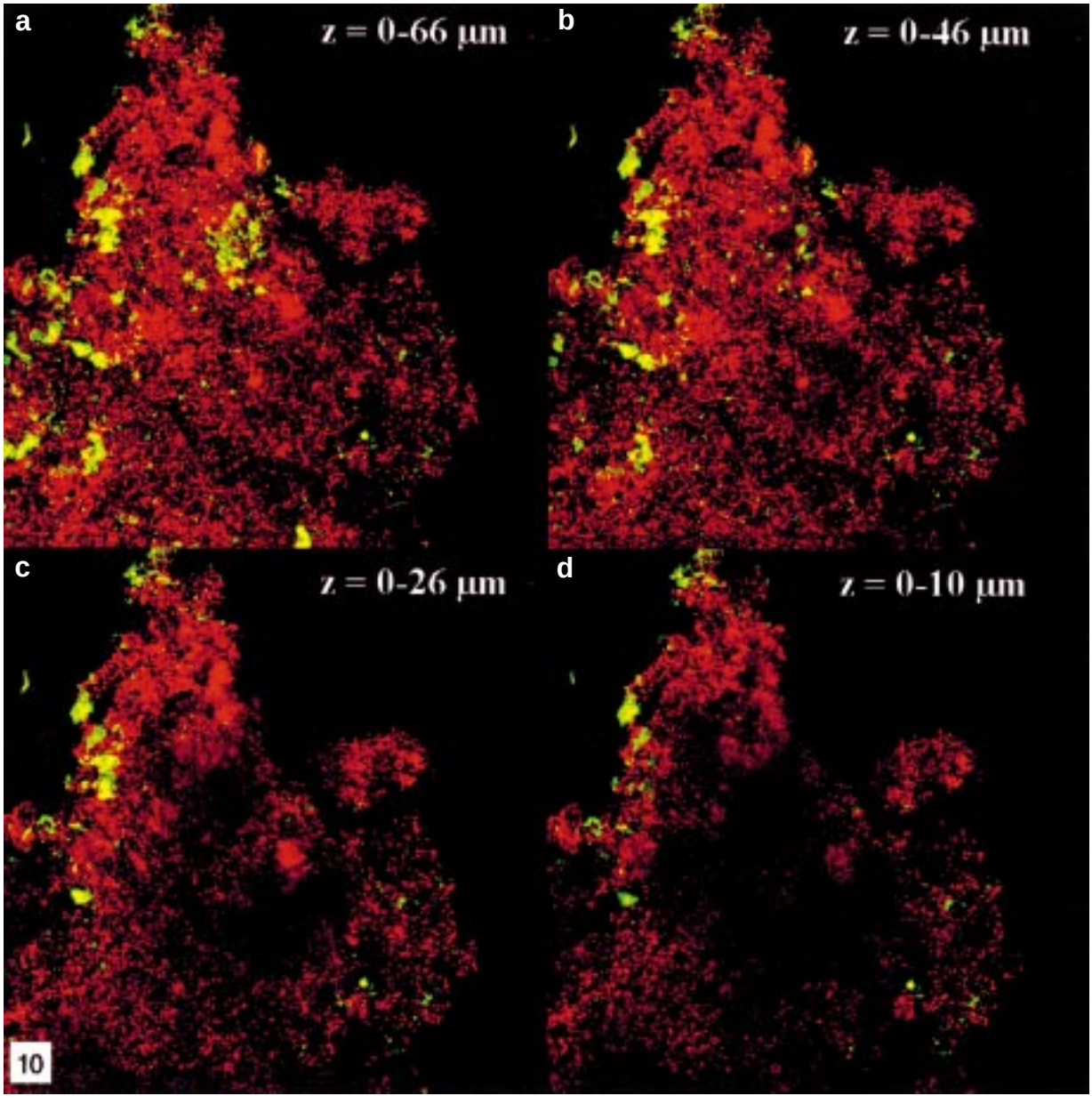

Figure 2 CLSM analysis of a 36-day-old biofilm grown on a stainless steel coupon ennobled in Baltic Sea water. The steel coupon was stained with EtBr (red) and fluorescent latex beads (green, aldehyde sulfate Fluospheres™, diameter 0.02 μm). Panel (a) shows a 66-μm-thick cell cluster on stainless steel surface (black). The projection (*xy*) was calculated with the look-through method from 132 single *xy*-sections (*z*-step 0.5 μm). Panels (b), (c) and (d) show 46-μm (b), 26-μm (c) and 10-μm (d) thick biofilm slices (*xy*) proximal to the steel surface. These projections reveal a dye non-penetrated area inside the cell cluster. Scalebox 10 μm.

is a membrane-permeable phenanthridinium stain with nucleic acid intercalator properties. Its calculated log K_{ow} is –0.38 at pH 7. Other nucleic acid targeted dyes, SYTO 16 and acridine orange (calculated log K_{ow} 1.24) penetrated less than EtBr, SYTO 16 only to $\leqslant$7 μm (Table 3). Log K_{ow} of SYTO 16 was measured as 1.48, indicating it is 72 times more soluble in *n*-octanol than EtBr. The EtBr stained in 15 min a zone corresponding to $>$10 cells in a stack, SYTO 16 less than five cells in a stack. The deepest penetration for EtBr of the three nucleic acid stains may be related to differences in polarity: hydrophilic compounds may have better access into the interior of the biofilm clusters on ennobled stainless steel in Baltic Sea water than the more hydrophobic compounds.

After extending the staining time to 6 h, the cores of the biofilm clusters remained unstained, but the volume of the unstained core had shrunk from 25% to $<$5% of the volume for a cluster size of ~100 μm in the basal diameter. The same staining protocol was used for *Mycobacterium gadium* NCTC 10942 and *Deinococcus geothermalis* RSPS-7a with lipid and protein layers as permeability barriers. Clumps of these cells stained fully in 15 min, thus the acid/alcohol fast cell wall (*M. gadium*) or the extensive S-layers (*D. geothermalis*, unpublished observations of

Table 3 Penetration of fluorescent dyes and beads into biofilm clusters on ennobled stainless steel in Baltic Sea water. Simultaneous staining with two dyes. For the composition of the stains, see Table 2. Dye penetration was calculated from individual *xy*-sections collected by CLSM using *z*-step 0.5 μm. The measured clusters had a basal diameter of 120–150 μm

Stain I	Penetration[a] (μm)	sdv[b]	*n*[c]	Stain II	Penetration (μm)	sdv	*n*	ID
CM 1.0 μm[d]	~1.00			CM 0.1 μm[d]	1.46	0.72	32	Va1
CM 0.1 μm	1.30	0.75	33	CM 0.02 μm	1.44	0.58	30	77a
CM 0.1 μm	1.58	0.83	41	ConA-TRITC	4.49	1.29	34	54a
CM 0.02 μm	0.72	0.28	24	AS 0.02 μm[e]	0.78	0.27	29	75a
CM 0.02 μm	1.26	0.61	16	AS 0.02 μm	1.02	0.55	22	74a
CM 0.02 μm	2.04	0.95	46	AS 0.02 μm	2.14	0.88	31	81a
CM 0.1 μm	1.09	0.45	8	EtBr[f]	>14.00			90a
CM 0.1 μm	1.55	0.67	54	EtBr	16.46	5.10	32	78a
AS 0.02 μm[e]	1.31	0.56	15	EtBr	5.19	2.22	14	83a
AS 0.02 μm	1.45	0.64	31	EtBr	17.02	5.55	29	80a
AS 0.02 μm	2.70	1.08	26	EtBr	11.86	2.96	16	87a
CM 0.02 μm	2.22	1.16	18	SYTO 16	6.73	2.89	20	79a

[a]Average of the measured penetration, staining time 15 min.
[b]Standard deviation.
[c]Number of measurements.
[d]Carboxylate-modified fluorescent latex beads.
[e]Aldehyde-sulfate fluorescent latex beads.
[f]As measured from the compact colony of morphologically similar cells seen in Figure 6.

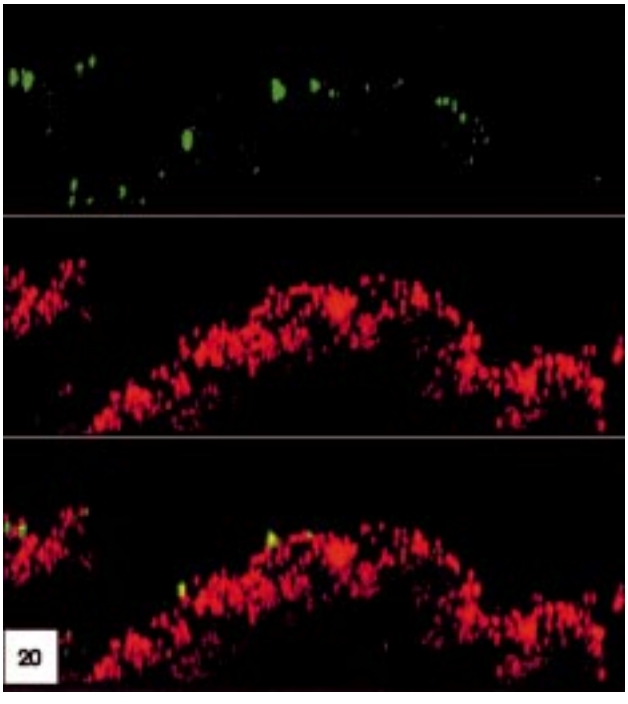

Figure 3 CLSM analysis of a 36-day-old biofilm grown on a stainless steel coupon ennobled in Baltic Sea water. Three *z*-projections of a biofilm cluster are shown, metal surface at the bottom of each projection. The upper panel shows the penetration of fluorescent latex beads (green, diameter 0.02 μm, aldehyde sulfate Fluospheres™), the middle panel shows ethidium bromide (red) with better penetration and the lowest panel shows the sum. Each projection represents a 10-μm-thick *z*-section of the cluster, calculated from 132 *xy*-scans (*z*-step 0.5 μm). Scalebox 20 μm.

M. Salkinoja-Salonen) did not exclude EtBr. Therefore, the cell clusters on ennobled stainless steel contained more efficient barrier material than the inspected strains of *Mycobacterium* and *Deinococcus*.

Table 3 shows similar depths of penetration for fluorescent beads of 0.02–1.0 μm in diameter. All the 0.02-μm beads, irrespective of functional properties or surface charge (Table 2) had similar penetration. Results from sequential staining were not different from simultaneous double staining. These results indicate the absence of accessible cavities inside the clusters. Figures 2 and 3 show that intercellular distances between EtBr-stained cells in the clusters ranged from 0.1 to 2 μm. The observation that this intercellular space was regularly not accessible even for the 0.02-μm beads, indicates the presence of an intercellular matrix. The results in Table 3 also show staining of the cell clusters with the concanavalin A lectin (ConA conjugated with tetramethylrhodamine fluorophore TRITC) to a depth of 4–5 μm, indicating accessible mannose and glucose residues at these depths in the cell clusters. In summary, the biofilm on ennobled stainless steel consisted of bacterial clusters with effective diffusion barriers towards dissolved dyes and beads close to colloid-size.

Patchiness of the living cell clusters on ennobled stainless steel

Fluorescent beads with different properties were used to analyse the surface quality of the living cell clusters. Figure 5 shows single *xy*-sections of a cluster <50 μm in height, after simultaneous staining with 0.02-μm aldehyde sulfate (hydrophobic) and carboxylate-modified (hydrophilic) fluorescent latex beads. Both types of beads adhered to peripheral areas of the clusters only, leaving the core unstained with no indication of deep voids. Table 3 shows that both beads penetrated to equal depths in the cluster (1.02 and 1.26 μm, respectively), but as is seen in Figure 5 the beads localized in different regions. This indicates patchiness of the biofilm surface, possibly due to different local populations of the surface-exposed bacteria. Similarly-differentiated surface areas can also be seen in Figures 2, 3 and 6, from the selective adherence of 0.02-

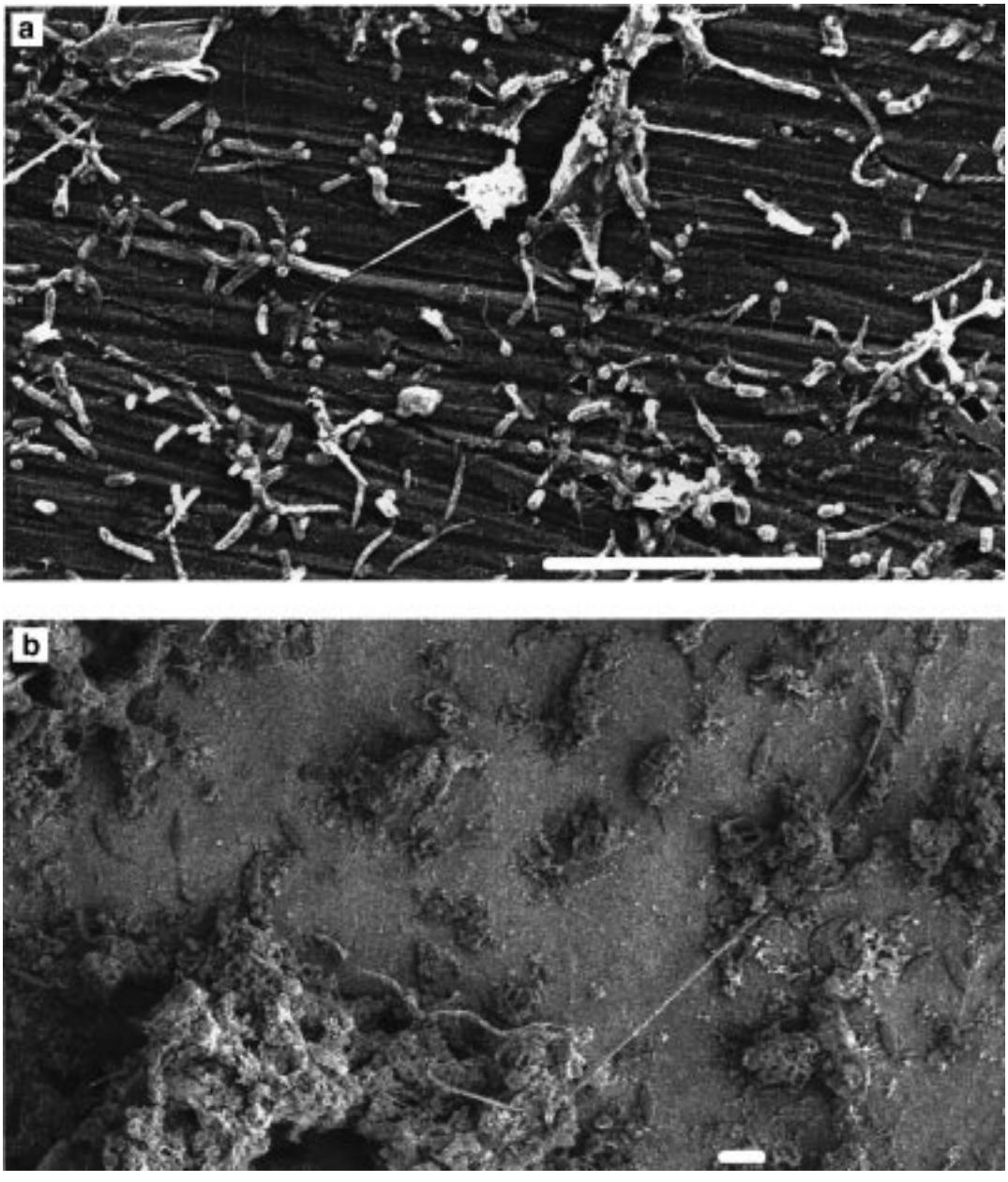

Figure 4 Scanning electron micrograph of stainless steel biofilms grown in Baltic sea water. Panel (a) shows morphologically different single bacteria adherent to the steel surface during the first 22 days of immersion. Panel (b) shows cell clusters on the ennobled stainless steel after 56 days of immersion (27 days after ennoblement). Scalebars 10 μm.

μm aldehyde sulfate beads and 0.1-μm carboxylate-modified beads, respectively. Panel (d) in Figure 5 represents the 2-μm layer closest to the steel, and shows scattered binding of both types of beads on areas of the steel surface surrounding the cluster, indicating the presence of a thin layer of biofilm close to the steel, accessible to the beads.

Figure 6 shows simultaneous staining with EtBr (red) and 0.1-μm carbodylate modified beads (green) of a 53-μm high cluster. As in Figure 2, EtBr-stained short rods are the most common cell type, but also filamentous bacteria are visible. Figure 6 displays a spherical colony ~30 μm in diameter composed of densely packed, morphologically similar rod-shaped bacteria (0.5 $\times$ 2–3 μm). The colony is located inside the cluster, surrounded by other types of cells. The hydrophilic 0.1-μm beads did not penetrate to such intraclustral colonies. Two types of intraclustral colonies of diameter 10–30 μm were regularly detected, the more common type contained rods as seen in Figure 6, the other type contained large cocci (2 μm). One cluster in the biofilm could contain one to three of such colonies. The bacteria inside the intraclustral colonies were in intimate contact, the local cell density reaching 10^8–10^9 cells mm^{-3}, 250–8000 cells in each intraclustral colony. The bulk cell density in the main cluster was 1–5 $\times$ 10^7 cells mm^{-3} and the EtBr-stained cells were surrounded by non-stained spacer material.

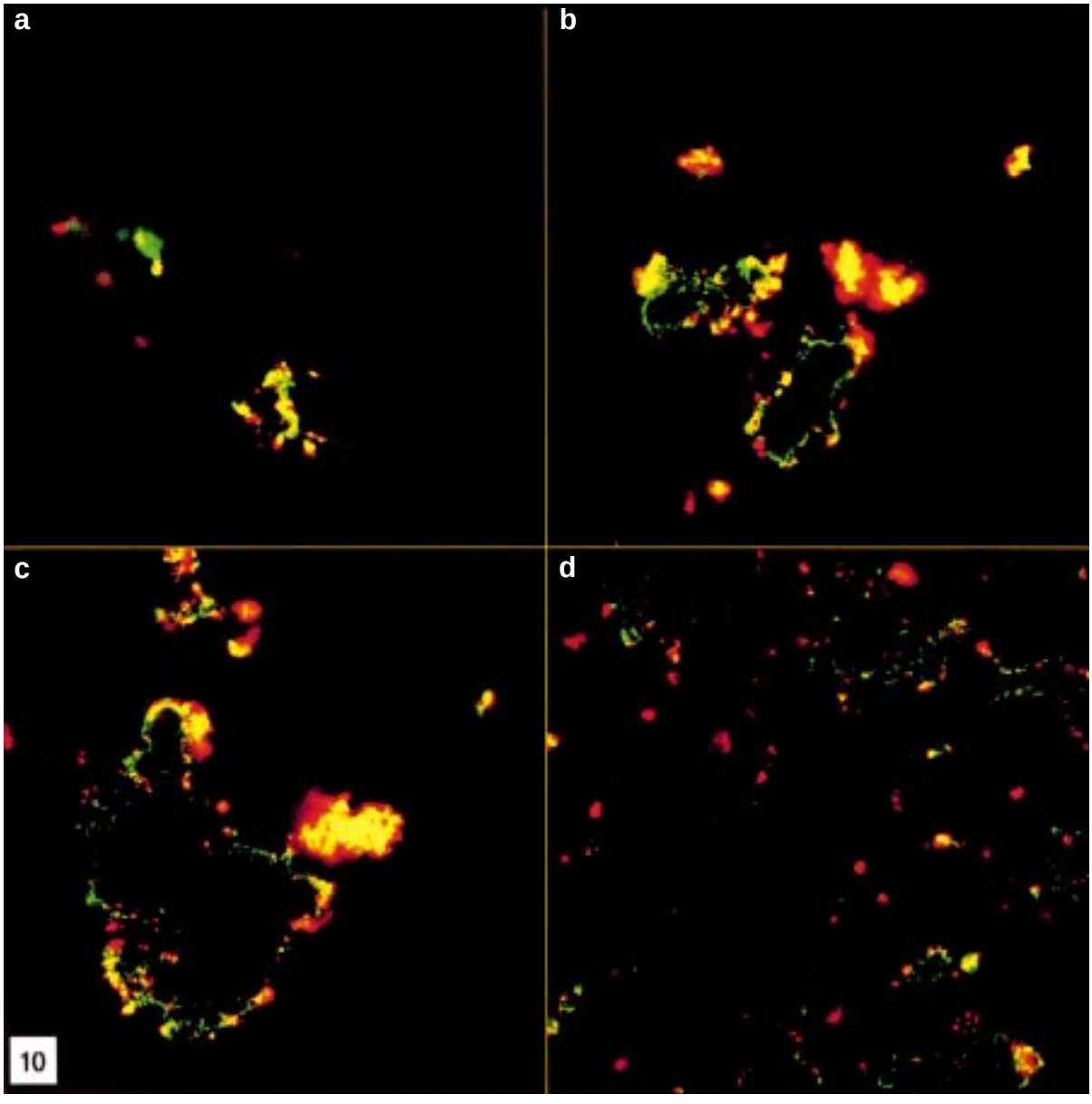

Figure 5 CLSM analysis of surface quality of the 36-day-old biofilm on ennobled stainless steel using 0.02-μm fluorescent latex beads as indicator. Simultaneous staining with aldehyde sulfate (green) and carboxylate-modified (red) beads revealed differently stained regions. Each panel shows a single *xy*-section, at distances of 46 μm (a), 32 μm (b), 21 μm (c) and 2 μm (d) distal to the steel surface. Scalebox 10 μm.

In conclusion (Figures 2–6, Table 3), the spatial and surface properties of cell clusters making up the biofilm on ennobled stainless steel surfaces were as follows: 15–20 clusters mm^{-2} covered cumulatively 10–20% of the surface; the interiors of the clusters were impermeable to the stains used. The impermeable core represented 25–45% (EtBr) or >95% (0.02-μm beads) of the total volume in a cluster ~100 μm in basal diameter. The absence of fluorescence signal from the core area was not an artifact caused by poor laser penetration, since diatoms trapped underneath the clusters were clearly visible by their red autofluorescence. Surfaces of the clusters contained differentiated regions, as hydrophobic and hydrophilic latex beads adhered to different peripheral regions of the clusters. The majority (>80%) of microbes in the inspected clusters on ennobled stainless steel were ⩽1 μm long rod-shaped bacteria. Longer rods (2–3 μm), coccoidal bacteria, filamentous microbes and diatoms were detected in lower density or as discrete, densely packed intraclustral colonies of morphologically similar bacteria. When the detected filamentous bacteria were examined with bigger magnification (zooming 3× with the CLSM), the proportions of rods in chain, cyanobacteria and sheathed cells characteristic of the *Leptothrix-Sphaerotilus* group of bacteria were 70%, 25–30% and <5%, respectively. Live amoebas and nematodes feeding on the biofilm biomass were occasionally detected. Dark brownish

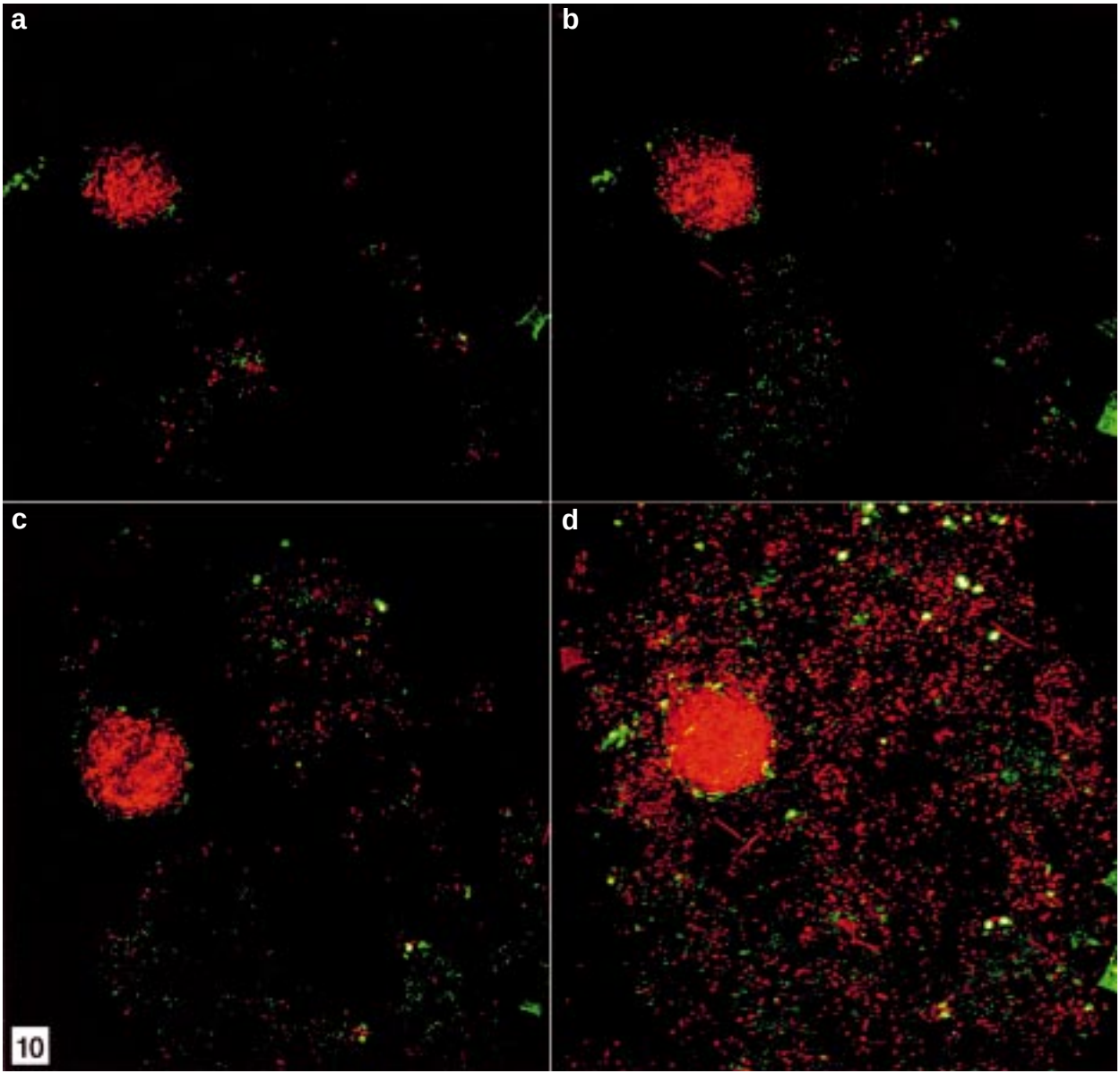

Figure 6 CLSM image showing heterogeny in biofilms grown on ennobled stainless steel for 36 days in Baltic Sea water. The coupon was stained with EtBr (red) and fluorescent latex beads (green, diameter 0.1 μm, carboxylate-modified Fluospheres™). Panels (a–c) show single *xy*-sections (0.5 μm) at distances of 38, 33 and 28 μm distal to the metal surface, revealing an internal colony of densely packed and morphologically similar bacteria. Panel (d) shows a projection of the whole 53-μm thick cluster, revealing the location of the dense bacterial colony. Scalebox 10 μm.

inorganic particles of diameter 10–15 μm embedded in the biofilms were regularly seen.

Microbiological diversity of biofilms on ennobled stainless steel

Live Gram-stain was used to distinguish living Gram-positive from Gram-negative bacteria in the biofilms grown in Baltic Sea water without losing information on the cell location in the 3-D biofilm matrix. Figure 7 is the sum of three subsequent confocal *xy*-sections (*z*-step 0.5 μm), showing a cluster containing scattered green colored cells indicating live Gram-negative bacteria flanked by red colored individual cells (Gram-positive status or cells at a low state of metabolic activity). Unstained matter physically separated the individual cells. Inside the cluster one internal colony of bacteria is visible, compactly packed with cocci. Peripheral cells of the intraclustral colony show a Gram-negative staining pattern, while the innermost cells show colocalized fluorescence interpretable as Gram-negative non-viable cells or cells at a low state of metabolic activity. The majority of the live cells on ennobled stainless steel had Gram-negative staining behavior.

Phylogenetic stains (Table 1) were used to analyze microbiological diversity in the biofilms on ennobled stainless steel. Figure 8 shows four CLSM projections, built from 20 optical *xy*-sections each. Panel (a) shows the pattern obtained after hybridization with the bacterial probe EUB338 (green) and gamma *Proteobacteria*-targeted probe

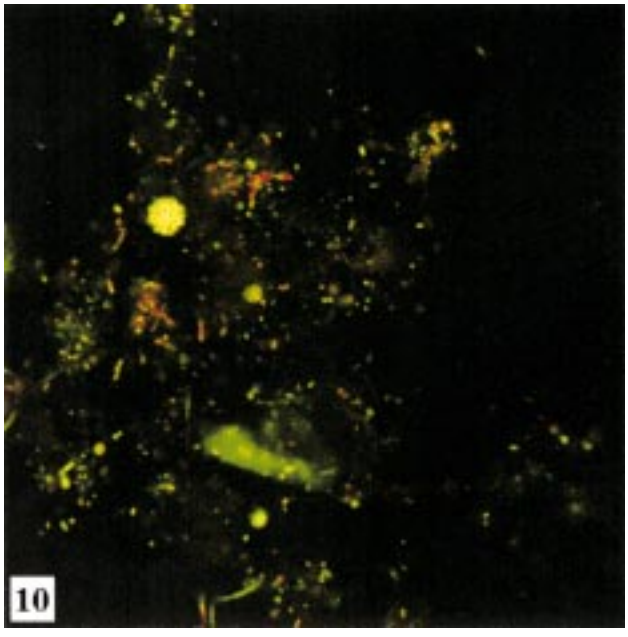

Figure 7 CLSM analysis of Gram-stained living biofilm grown on ennobling stainless steel for 36 days. The figure shows a projection built with the maximum intensity method from three *xy*-scans with *z*-step 0.5 μm near the top of the cell cluster. The green color (SYTO 9) indicates the presence of Gram-negative living bacteria and the yellow or red color (SYTO 9 + hexidium iodide or just hexidium iodide, respectively) indicates Gram-positive bacteria, dead bacteria or eucaryotes. Scalebox 10 μm.

GAM42a (red). In all coupons the majority of hybridized bacteria were green-fluorescing short (<2 μm) rods or cocci, labeled with the bacterial probe only. Filamentous organisms in panel (a) are cyanobacteria labeled with the bacterial probe only, recognized from the patterns in yellow fluorescence ie colocalized green and red signal, where the red autofluorescence originates from photosynthetic pigments. In panel (a) the hybridization conditions were optimized according to the GAM42a probe, demanding more stringent conditions than the EUB338 probe (Table 1). The high stringency may have left a part of the bacteria unlabeled and a few bacteria were clearly labeled only with the GAM42a probe and showed red fluorescence instead of yellow, as it should if hybridized with both probes. In summary, from all hybridized bacteria $<15\%$ hybridized with the GAM42a probe, indicating they belonged to the gamma group of *Proteobacteria*.

Panels (b–d) in Figure 8 show the results of simultaneous hybridization with the bacterial probe EUB338 (green) and alpha *Proteobacteria*-targeted probe ALF1b (red). Panel (d) is a close-up of the cluster visible in the central part of panel (c). Panel (b) shows a group of *ca* 30 red coccoidal cells ~2 μm in diameter and panels (c) and (d) show short rods with red fluorescence. These cells thus had hybridized with the ALF1b probe only. A database search showed that 11.8% of the bacterial 16S rRNA sequences currently in databases match perfectly with ALF1b probe, but had one to four mismatches with the bacterial probe EUB338. The conditions used for hybridization were similarly stringent for both probes (Table 1), therefore bacteria with mismatches were likely to remain unlabeled with EUB338. Examples of such taxa are listed in Table 4. Some clusters showed regions, where the adjacent bacteria all had green fluorescence (arrows in panels (b) and (d)), thus hybridized with the bacterial probe EUB338 only, and regions where the adjacent bacteria all had yellow fluorescence indicative of binding of both probes. In some regions of the cluster adjacent cells showed heterogenic hybridization patterns. Spherical intraclustral colonies of compactly packed cells (up to 10^9 mm^{-3}) with morphologically similar bacteria as the one marked with an arrow in panel (d) were regularly seen. These intraclustral colonies had intensive green fluorescence and thus were labeled with the bacterial probe only. The bacteria binding the ALF1b probe represented 25–30% of all bacteria stainable with the bacterial probe.

Figure 8 shows the 3-D structure of the dehydrated biofilms on ennobled stainless steel. The clusters were flattened to 10–20 μm in height as compared to >50 μm in the living biofilms at their native hydrated state shown in Figures 2, 3, 5, 6 and 7. In contrast to live biofilms (Figures 2, 3, 5, 6 and 7), the cells inside the clusters were stained and no unstained core was found. Fluorescence of the innermost cells was weak, indicating low cellular RNA contents or poor penetration.

Colonies inside clusters were observed by each of the three techniques used: by combined EtBr-microbead staining (Figure 6) and by live Gram-staining (Figure 7) in living biofilms, and also in fixed, dehydrated biofilms by phylogenetic staining (Figure 8). Adding up the information from these techniques, the intraclustral colonies were 10–30 μm in diameter, composed of Gram-negative bacteria not belonging to alpha or gamma *Proteobacteria* and with an activity gradient decreasing from surface towards the core. Nematodes were regularly seen in unstained samples by their autofluorescence. In hybridized samples (arrow in panel (c)), the fluorescence of nematodes was further enhanced when the bacteria-filled guts bound the oligonucleotide probes. In addition to hybridization signals, autofluorescing diatoms of the *Navicula*-resembling bilateral type independently adhering to the stainless steel surface were sometimes seen (panels (b) and (c)).

Discussion

An increase of the open circuit potential of stainless steel (ennobling) is considered to represent the first step of microbially influenced corrosion. We studied biofilms on ennobled stainless steel in natural Baltic Sea water using CLSM in combination with different functional stains to analyze the 3-D structure, permeability barrier properties and microbial community structure. This is an extension of our earlier work where stainless steels were for the first time shown to ennoble similarly to field conditions in a laboratory ecosystem simulating the Baltic Sea. We are not aware of other reports on microbial communities of the Baltic Sea (brackish water) biofilms on ennobled stainless steel. As marine bacteria are often non-cultivable [2] and the *in situ* hybridization can reveal the spatial distribution and activity of taxonomic groups of bacteria in multispecies biofilms [35,40], fluorescently labeled rRNA targeting oligonucleotide probes were applied. We used probes for alpha and gamma subclasses of the *Proteobacteria*, as

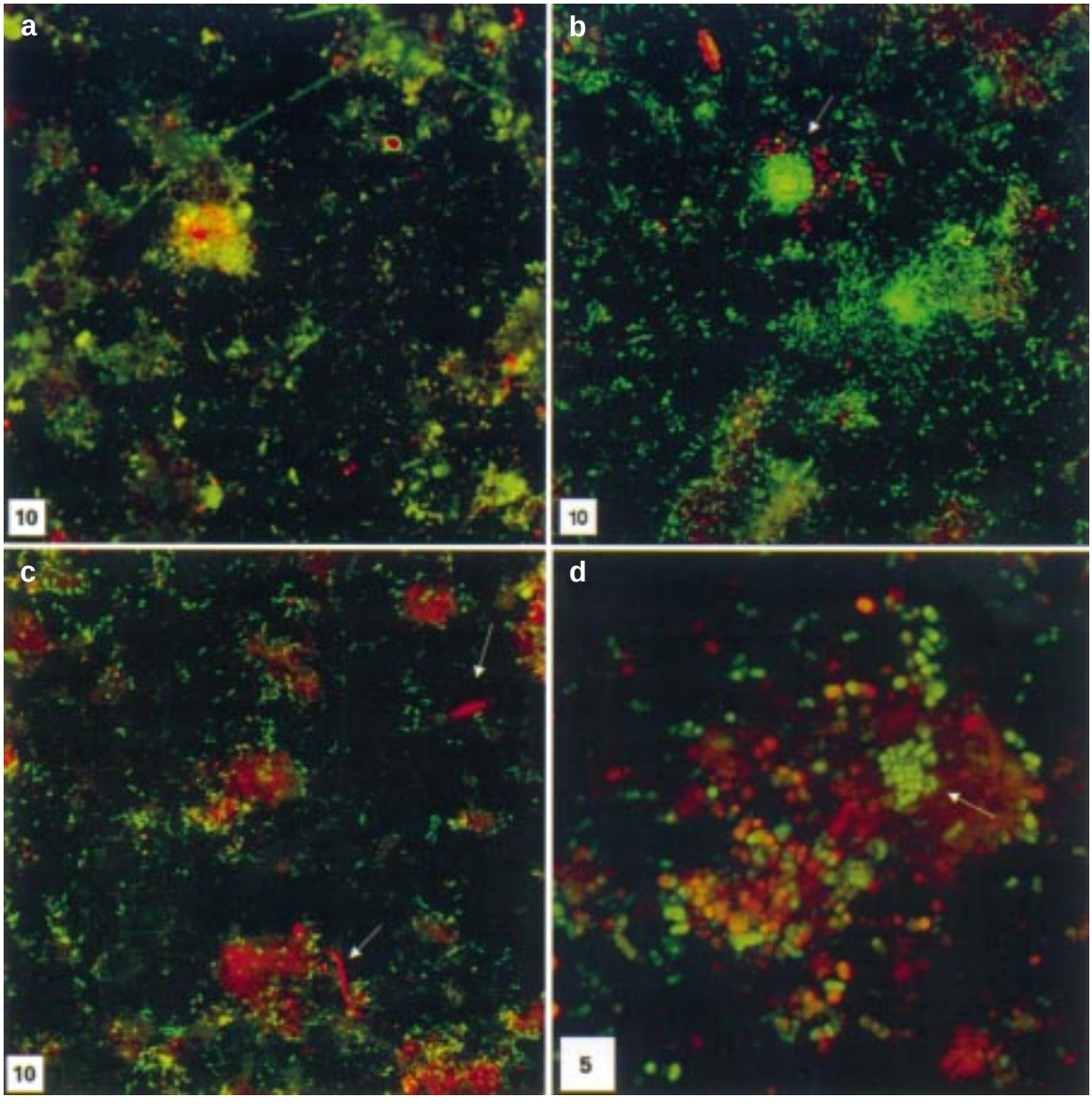

Figure 8 CLSM images of a 30-day-old biofilm on ennobled stainless steel hybridized *in situ* with phylogenetic stains EUB338 (targeted for the bacteria), GAM42a (gamma group of *Proteobacteria*) and ALF1b (alpha group of *Proteobacteria*). Targeted specificities of the probes are shown in Table 1. The green color indicates cells hybridizing with the EUB338 probe. Panel (a): the red color (Cy3) shows cells labeled with the probe GAM42a. Panels (b–d): the red color reveals cells labeled with probe ALF1b. Cells hybridizing with the ALF1b were twice as abundant as cells hybridizing with the GAM42a. Projections were calculated with the maximum intensity method from 20 *xy*-sections collected with *z*-step of 0.5 μm. Scalebox 5 or 10 μm.

sequences from both subclasses have been commonly retrieved from the marine picoplankton [2]. In this paper we report: (i) on the spatial and biological structure in the biofilm community on ennobling stainless steel; and (ii) on the phylogenetic and permeability properties of such biofilms on ennobled stainless steel surfaces. We performed the *in situ* hybridization directly on steel, with no mechanical disturbance of the biofilm community. To our knowledge there are no earlier published reports in this area.

The analyzed stainless steel coupons ennobled with a shift in the E_{corr} from −200 to −100 mV to +300 to +400 mV_{SCE} after immersion for 3–4 weeks in Baltic Sea water [33]. Our study showed that the post-ennoblement biofilm on stainless steel consisted of individual clusters of bacteria covering 10–20% of the steel surface, generally extruding <100 μm from the steel surface and consisting mainly of bacteria, $1–5 \times 10^7$ cells mm^{-3}. Transmission electron microscopic study of the clusters, published elsewhere [33], also showed that the unstained core of the clusters consisted of densely packed bacteria. Dissolved dyes revealed dye non-penetrated interiors of the clusters comprising 25–95% of the volume of each cluster, *ca* 100 μm in diameter. There were no measurable voids inside the clusters and the mass transport inside the clusters seemed to be governed by molecular diffusion only.

The biofilms in the present study grown in oligotrophic

Table 4 Examples of bacterial strains with a perfect match of the 16S rDNA sequence with ALF1b probe and mismatches with bacterial probe EUB338. The examples were selected on the basis of possible relevance for oligotrophic environments. The listed taxa may be expected to show up in phylogenetic staining using ALF1b probe, but not with EUB338 probe (see Figure 8)

Bacterial strain	Mismatches to EUB338	GenBank accession No.	Description	Isolation source	Reference
Caulobacter cresentus CB2	1	X52281	stalked α-proteobacteria	bacterioplankton, Sargasso sea	[19]
Caulobacter sp FWC17	1	M83801	stalked α-proteobacteria	waste water treatment plant	[44]
Caulobacter sp FWC18	2	M83802	stalked α-proteobacteria	waste water treatment plant	[44]
Methylocystis pyriformis 14	1	L20803	α-proteobacteria, methanotroph group IIa		[9]
Methylosinus sp strain B	4	M95663	α-proteobacteria, methanotroph group IIa		[7]
Methylosporovibrio methanica 81Z	3	M29025	α-proteobacteria, methylotroph group II		[45]
Methylocystis minimus 42	2	L20844	α-proteobacteria, methanotroph group IIa		[9]
Gemmata obscurilobus UQM 2246 (ACM 2224)	3	X54522 X56305	Planctomycetales, budding bacteria	lake water, Australia	[17,27]
Acidosphaera rubrifaciens HS-AP3	2	D86512	α-proteobacteria, phototroph		
Sphingomonas aromaticivorans SMCC B0522	1	U20774	*Zymomonas* group of α-proteobacteria	deep subsurface sediments	[18]
Rhodospirillum sodomense DSI	1	M59072	α-proteobacteria, oblig. halophilic, anoxygenic phototroph	water/sediment of the Red Sea	[30]
Spirochaeta bajacaliforniensis BA2	1	M71239	Sphirochaetales	microbial mat community, Laguna Figueroa, Mexico	[16]
Unknown (9 soil clones)	1–2	X65374–X64382		soil, Australia	[26]
Bradyrhizobium sp 55S	2	D14507	α-proteobacteria	leguminous plant, Philippines	[39]

Baltic Sea water resembled the consensus model for biofilms described by Costerton *et al* [11], in the sense that between the clusters there was free access for sea water to the steel surface. However, our data show the virtual absence of water channels inside the biofilm clusters. This key finding clearly distinguishes the ennobling biofilms on stainless steel from the consensus model.

We used CLSM and worked with living stained biofilms, which yielded a close-to-reality picture of the biofilm structure and bacterial amounts on the ennobled stainless steel. Each cluster *ca* 100 μm in diameter contained ~10^4 bacteria and there were 5–20 such clusters mm^{-2} ie 0.5–2 $\times$ 10^5 cells mm^{-2}. Only 10^3 bacteria mm^{-2} were cultivable on Plate Count Agar from biofilms on parallel coupons, scraped off with an alginate swab [10], indicating a yield of $<$2% of the biofilm bacteria. Concanavalin A conjugate stained the cell clusters to a depth of 4–5 μm (Table 3), indicating the presence of polymers with α-d-mannose and/or α-d-glucose residues. Extracellular matrix is assumed to be important for the survival of attached communities [24].

Microelectrode studies have shown concentration gradients in biofilms for oxygen [5,41] and nutrients [42]. Lawrence *et al* [25] and Møller *et al* [36] used fluorescent dextrans with defined charges and molecular sizes in conjunction with CLSM to study the charge distribution of polymers and permeability properties within biofilms and showed regional variability in the binding and motility of the dextrans. We used as a new tool fluorescent beads of near-to-colloid-sizes, 0.02 and 0.1 μm, to study the porosity and the surface polarity of biofilms. The 0.02-μm carboxylate-modified beads with a negative surface charge (16.1 μC cm^{-2}) are hydrophilic, while the 0.02-μm aldehyde sulfate beads have a lower negative charge (4.2 μC cm^{-2}) and are hydrophobic. Both 0.02-μm beads penetrated similarly into the living cell clusters, but adhered to clearly different surface locations (Figure 5), indicating nonrandom heterogeneity of the surface, explainable by different local populations of the surface-exposed bacteria. When studying the porosity of wastewater reactor biofilms, Okabe *et al* [38] found that larger latex beads of diameter 1 μm (carboxylate modified, negative surface charge) traversed throughout a 360-μm thick biofilm in less than 23 min by advective transport via the voids and pores in the biofilm matrix. Similar beads were also used by de Beer *et al* [5] with reactor-grown mixed population biofilms on cover glass. In both studies the biofilms also contained clusters not penetrated by the beads, surrounded by areas composed of water channels, voids and sparse polymeric material. Our results showed that the beads had free access to areas of metal surface not occupied by bacterial clusters, but the penetration was $<$2 μm even for 0.02-μm beads, independent of the surface polarity. In aqueous solutions the 0.02-μm beads behave very much like colloids [21]. The distance between the nucleic acid-stainable areas of bacteria in the clusters was 10–100 times wider than the diameter of the beads used. The poor penetration of the beads into this space (Table 3) indicates transport barriers, for instance the presence of intercellular material, the absence of free water between adjacent cells, or positive electric charges on cell or matrix surfaces preventing the transport of the negatively charged beads by electrostatic forces. The most hydrophilic of the nucleic acid stains used in this study, EtBr (log K_{ow} −0.38) penetrated deepest (Table 3), suggesting that hydrophilic compounds may have more free access into the ennobling Baltic Sea microbial community on

stainless steel. This was a uniform property of the living bacterial clusters on the ennobled steel surfaces.

The drawback of the *in situ* hybridization protocol is the dehydration step, causing compression of the clusters to 15–20% of the original height (this study) or more [35]. Despite this compression, phylogenetically different bacteria were distinguishable in separate regions inside the clusters. Similarly, analysis of living biofilms showed discrete microbial groups inside the clusters and heterogeny in the surface functionality. Live Gram-staining indicated that in the thoroughly-stained compact intraclustral colonies of bacteria the peripheral cells were more active, and they also gave stronger hybridization intensity than cells in the interior, probably indicating a higher rRNA content and a higher state of metabolic activity [35,40]. A similar gradient towards the core was observed in *Pseudomonas* monoculture biofilms [22,23].

Results of live Gram-staining and hybridization techniques in this study indicated that Gram-negative bacteria were the dominant organisms in the Baltic Sea biofilms on ennobled stainless steel. Cells hybridizing with probe targeted to alpha *Proteobacteria* were twice as abundant as cells responding to the gamma-*Proteobacteria* probe. Despite equal stringency of hybridization conditions for probes ALF1b and EUB338, a significant quantity of bacteria binding ALF1b, but not to the EUB338 probe were detected, as shown in Figure 8 panel (d). A search in 16S rRNA sequences currently in databases (Ribosomal Database Project [31] and GenEMBL) revealed that 11.8% of the sequences having a perfect match with ALF1b probe had one to four mismatches with bacterial probe EUB338. Table 4 lists examples of such taxa. For instance *Methylocystis pyriformis* 14 and *M. minimus* 42 are candidates to explain the red-only fluorescing cocci in Figure 8 (b) and (d). The interiors of dense biofilms were suggested to be occupied by anaerobic bacteria in recent biofilm models [5,11,14,24]. Anaerobic bacteria oxidizing multicarbon compounds while reducing iron or some other metals, eg *Geobacter metallireducens* ATCC 53744 [29], belong to the delta *Proteobacteria*, but have a perfect match with the ALF1b probe and could be seen as yellow-fluorescing cells in Figure 8 (b–d). Such bacteria may contribute to cathodization of the steel during ennoblement and later to destruction of the passive layer on stainless steel leading to corrosion.

Several studies have shown coupling between biofilm formation and ennoblement [12–14,33,34,43]. Dickinson *et al* [13] proposed a model of a stainless steel corrosion process, where several multicellular units of specialized bacteria act synergistically resulting in ennoblement and pit corrosion. The model includes heterotrophic manganese- and iron-oxidizing bacteria (MFOB) colonizing the stainless steel surface and producing MnO_2-rich deposits. This biomineralization of manganese may increase the potential and the cathodic current density observed during ennoblement. The MnO_2-rich deposits oxidize natural polymeric substances to organic substrates, beneficial for the activity of sulfate-reducing bacteria (SRB) lowering redox potential in the oxygen-depleted interior of the cluster. As the MnO_2 deposits prevent repassivation of the stainless steel in nucleation sites, the combined action of MFOB and SRB promote pit corrosion. Linhardt [28] demonstrated that even minute amounts of MnO_2 attached to the surface may have a considerable influence on E_{corr} of stainless steel. Many bacteria can oxidize manganese, including the filamentous bacteria *Leptothrix* and *Sphaerotilus*; budding or appendaged bacteria *Caulobacter*, *Gallionella*, *Hyphomonas*, *Hyphomicrobium* and *Pedomicrobium*; strains of *Arthrobacter*, *Bacillus*, *Chromobacterium*, *Micrococcus*, *Oceanospirillum*, *Burkholderia*, *Siderocapsa* and *Vibrio* [13,20]. The rate of bacterial manganese oxidation is enhanced by the biofilm mode of growth [37]. CLSM showed the presence of filamentous bacteria in the biofilms (Figures 2, 6, 7 and 8) and bacteria resembling *Caulobacter* and *Hyphomonas* were revealed with SEM (Figure 4). The 16S rRNA targeted probe used, ALF1b, matches perfectly with several strains of *Caulobacter* and *Pedomicrobium* strains and also with several SRBs, although these belong to the delta *Proteobacteria* [32]. Our observations show that the bacterial clusters on ennobled stainless steel were diffusion-limited, had differentiated surfaces and a microscopic architecture allowing for development of different oxidation-reduction environments. Dickinson *et al* [13] presented a functional model for the ennobling biofilm on stainless steel with different oxidation-reduction environments inside the same biofilm cluster. Our phylogenetic data on the composition of the biofilm bacterial community and the patchy structure of the bacterial clusters can accommodate bacterial taxa capable of carrying out the redox reactions as suggested in the Dickinson model. The Baltic Sea water used in our study contained humic substances (4–7 mg of DOC L^{-1} [33]) which are oxidizable by MnO_2 deposits and then usable by methylotrophs and other microbes in the multispecies biofilm, and may provide suitable substrates for the growth of SRB and Fe^{3+} reducing bacteria. The stainless steel in Baltic Sea water was ennobled with a shift in the E_{corr} near to +350 mV_{SCE} [33], similar to the E_{corr} fixed by the reactions of redox couple MnO_2-MnOOH [14]. Our results represent microscopic description of an ennobling biofilm, where the ennoblement could follow the sequence of redox events as suggested by the model of Dickinson *et al* [13].

Acknowledgements

This work was supported by the Center of Excellence Fund of Helsinki University, TEKES (COST 511 project), Outokumpu Polarit Oyj, Neste Oy and the Academy of Finland. We thank Leena Carpén and Tero Hakkarainen of VTT Manufacturing Technology and Aimo Saano and Riitta Vuorio for their cooperation.

References

1 Amann RI, J Stromley, R Devereux, R Key and DA Stahl. 1992. Molecular and microscopic identification of sulfate-reducing bacteria in multispecies biofilms. Appl Environ Microbiol 58: 614–623.
2 Amann RI, W Ludwig and K-H Schleifer. 1995. Phylogenetic identification and *in situ* detection of individual microbial cells without cultivation. Microbiol Rev 59: 143–169.
3 American Society for Testing and Materials. E 1147-92. Standard test method for partition coefficient (n-octanol/water) estimation by liquid chromatography. Annual Book of ASTM Standards, PA, USA. Vol. 14.01, pp 712–715.

4 Anonymous. 1995. Marine biofilm on stainless steels: effects, monitoring and prevention. Report on the European research project BIOFILM, contract No. MAS-CT92-0011, 13 pp.
5 de Beer D, P Stoodley, F Roe and Z Lewandowski. 1994. Effects of biofilm structures on oxygen distribution and mass transport. Biotechnol Bioeng 43: 1131–1138.
6 Borenstein SW. 1994. Microbiologically Influenced Corrosion Handbook. Woodhead Publishing, Cambridge, UK, 288 pp.
7 Bratina BJ, GA Brusseau and RS Hanson. 1992. Use of 16S rRNA analysis to investigate phylogeny of methylotrophic bacteria. Int J Syst Bacteriol 42: 645–648.
8 Braun-Howland EB, S Danielsen and SA Nierzwicki-Bauer. 1992. Development of a rapid method for detecting bacterial cells *in situ* using 16S rRNA-targeted probes. BioTechniques 13: 928–933.
9 Brusseau GA, E Bulygina and R Hanson. 1994. Phylogenetic analysis and development of probes for differentiating methylotrophic bacteria. Appl Environ Microbiol 60: 626–636.
10 Carpén L, L Raaska, K Mattila, MS Salkinoja-Salonen and T Hakkarainen. 1997. Laboratory simulation with natural bacteria populations. European Federation of Corrosion, publication no. 22, pp 113–122, The Institute of Materials, London, UK.
11 Costerton JW, Z Lewandowski, D DeBeer, D Caldwell, D Korber and G James. 1994. Biofilms, the customized microniche. J Bacteriol 176: 2137–2142.
12 Dexter S. 1995. Effect of biofilms on marine corrosion of passive alloys. In: Bioextraction and Biodeterioration of Metals (C Gaylarde and H Videla, eds), pp 129–168, Cambridge University Press, Cambridge, UK.
13 Dickinson WH and Z Lewandowski. 1996. Manganese biofouling and the corrosion behavior of stainless steel. Biofouling 10: 79–93.
14 Dickinson WH, F Caccavo, B Olesen and Z Lewandowski. 1997. Ennoblement of stainless steel by the manganese-depositing bacterium *Leptothrix discophora*. Appl Environ Microbiol 63: 2502–2506.
15 Ferreira AC, M Nobre, FA Rainey, MT DaSilva, R Wait, J Burghardt, AP Chung and MS DaCosta. 1997. *Deinococcus geothermalis* sp nov and *Deinococcus murrayi* sp nov, two extremely radiation resistant and slightly thermophilic species from hot springs. Int J Syst Bacteriol 47: 939–947.
16 Fracek SP and JF Stolz. 1985. *Spirochaeta bajacaliforniensis* sp nov from a microbial mat community at Laguna Figueroa, Baja California Norte, Mexico. Arch Microbiol 142: 317–325.
17 Franzmann PD and VB Skerman. 1984. *Gemmata obscuriglobus*, a new genus and species of the budding bacteria. Antonie van Leeuwenhoek 50: 261–268.
18 Fredrickson JK, D Balkwill, G Drake, M Romine, D Ringelberg and DC White. 1995. Aromatic-degrading *Sphingomonas* isolates from the deep subsurface. Appl Environ Microbiol 61: 1917–1922.
19 Giovannoni SJ, T Britschigi, C Moyer and KG Field. 1990. Genetic diversity in Sargasso Sea bacterioplankton. Nature 345: 60–62.
20 Gounot A. 1994. Microbial oxidation and reduction of manganese: consequences in groundwater and applications. FEMS Microbiol Rev 14: 339–350.
21 Haugland RP. 1996. Molecular Probes: Handbook of Fluorescent Probes and Research Chemicals. Molecular Probes Inc, Eugene, OR, USA.
22 Kinniment SL and JWT Wimpenny. 1992. Measurements of the distribution of adenylate concentrations and adenylate energy charge across *Pseudomonas aeruginosa* biofilms. Appl Environ Microbiol 58: 1629–1635.
23 Korber DR, G James and JW Costerton. 1994. Evaluation of fleroxacin activity against established *Pseudomonas fluorescens* biofilms. Appl Environ Microbiol 60: 1663–1669.
24 Korber DR, JR Lawrence, HM Lappin-Scott and JW Costerton. 1995. Growth of microorganisms on surfaces. In: Microbial Biofilms (HM Lappin-Scott and JW Costerton, eds), pp 15–45, Cambridge University Press, Cambridge.
25 Lawrence JR, GM Wolfaardt and DR Korber. 1994. Determination of diffusion coefficients in biofilms by confocal laser microscopy. Appl Environ Microbiol 60: 1166–1173.
26 Liesack W and E Stackebrandt. 1992. Occurrence of novel groups of the domain *Bacteria* as revealed by analysis of genetic material isolated from an Australian terrestrial environment. J Bacteriol 174: 5072–5078.
27 Liesack W, R Söller, T Stewart, H Haas, S Giovannoni and E Stackebrandt. 1992. The influence of tachytelically (rapidly) evolving sequences on the topology of phylogenetic trees—intrafamily relationships and the phylogenetic position of *Planctomycetaceae* as revealed by comparative analysis of 16S rRNA sequences. Syst Appl Microbiol 15: 357–362.
28 Linhardt P. 1997. Corrosion of metals in natural waters influenced by manganese oxidizing microorganisms. Biodegradation 8: 201–210.
29 Lovley DR, SJ Giovannoni, DC White, JE Champine, EJP Phillips, YA Gorby and S Goodwin. 1993. *Geobacter metallireducens* gen nov sp nov, a microorganism capable of coupling the complete oxidation of organic compounds to the reduction of iron and other metals. Arch Microbiol 159: 336–344.
30 Mack EE, L Mandelco, CR Woese and MT Madigan. 1993. *Rhodospirillum sodomense*, sp nov, a Dead Sea *Rhodospirillum* species. Arch Microbiol 160: 363–371.
31 Maidak BL, G Olsen, N Larsen, R Overbeek, MJ McCaughey and CR Woese. 1997. The RDP (Ribosomal Database Project). Nucleic Acids Res 25: 109–111.
32 Manz W, R Amann, W Ludwig, M Wagner and K-H Schleifer. 1992. Phylogenetic oligodeoxynucleotide probes for the major subclasses of proteobacteria: problems and solutions. Syst Appl Microbiol 15: 593–600.
33 Mattila K, L Carpén, T Hakkarainen and MS Salkinoja-Salonen. 1997. Biofilm development during ennoblement of stainless steel in Baltic Sea water: a microscopic study. Int Biodet Biodegrad 40: 1–10.
34 Mollica A. 1992. Biofilms and corrosion on active-passive alloys in seawater. Int Biodet Biodegrad 29: 213–229.
35 Møller S, AR Pedersen, L Poulsen, E Arvin and S Molin. 1996. Activity and three-dimensional distribution of toluene-degrading *Pseudomonas putida* in a multispecies biofilm assessed by quantitative *in situ*-hybridization and scanning confocal laser microscopy. Appl Environ Microbiol 62: 4632–4640.
36 Møller S, DR Korber, G. Wolfaardt, S Molin and DE Caldwell. 1997. Impact of nutrient composition on a degradative biofilm community. Appl Environ Microbiol 63: 2432–2438.
37 Nealson K and J Ford. 1980. Surface enhancement of bacterial manganese oxidation: implications for aquatic environments. Geomicrobiol J 2: 21–37.
38 Okabe S, T Yasuda and Y Watanabe. 1997. Uptake and release of inert fluorescence particles by mixed population biofilms. Biotechnol Bioeng 53: 459–469.
39 Oyaizu H, S Matsumoto, K Minamisawa and T Gamou. 1993. Distribution of rhizobia in leguminous plants surveyed by phylogenetic identification. J Gen Appl Microbiol 39: 339–354.
40 Poulsen LK, G Ballard and DA Stahl. 1993. Use of rRNA fluorescence *in situ*-hybridization for measuring the activity of single cells in young and established biofilms. Appl Environ Microbiol 59: 1354–1360.
41 Ramsing NB, M Kühl and BB Jørgensen. 1993. Distribution of sulfate-reducing bacteria, O_2, and H_2S in photosynthetic biofilms determined by oligonucleotide probes and microelectrodes. Appl Environ Microbiol 59: 3840–3849.
42 Schramm A, L Larsen, NP Revsbech, N Ramsing, R Amann and KH Schleifer. 1996. Structure and function of a nitrifying biofilm as determined by *in situ*-hybridization and the use of microelectrodes. Appl Environ Microbiol 62: 4641–4647.
43 Scotto V, M Beggiato, G Marcenaro and R Dellepiane. 1993. Microbial and biochemical factors affecting the corrosion behaviour of stainless steels in seawater. In: A Working Party Report on Marine Corrosion of Stainless Steels: Chlorination and Microbial Effect, pp 21–33, European Federation of Corrosion publication No. 10, The Institute of Materials, London, UK.
44 Stahl DA, R Key, B Flesher and J Smit. 1992. The phylogeny of marine and freshwater caulobacters reflects their habitat. J Bacteriol 174: 2193–2198.
45 Tsuji K, H Tsien, RS Hanson, S DePalma, R Scholtz and S LaRoche. 1990. 16S rRNA sequence analysis for determination of phylogenetic relationship among methylotrophs. J Gen Microbiol 136: 1–10.